Copyright Warning & Restrictions

The copyright law of the United States (Title 17, United States Code) governs the making of photocopies or other reproductions of copyrighted material.

Under certain conditions specified in the law, libraries and archives are authorized to furnish a photocopy or other reproduction. One of these specified conditions is that the photocopy or reproduction is not to be "used for any purpose other than private study, scholarship, or research." If a, user makes a request for, or later uses, a photocopy or reproduction for purposes in excess of "fair use" that user may be liable for copyright infringement,

This institution reserves the right to refuse to accept a copying order if, in its judgment, fulfillment of the order would involve violation of copyright law.

Please Note: The author retains the copyright while the New Jersey Institute of Technology reserves the right to distribute this thesis or dissertation

Printing note: If you do not wish to print this page, then select "Pages from: first page # to: last page #" on the print dialog screen

NJIT New Jersey's Science & Technology University

The Van Houten library has removed some of the personal information and all signatures from the approval page and biographical sketches of theses and dissertations in order to protect the identity of NJIT graduates and faculty.

ABSTRACT

DRUG RELEASING HYDROGELS FOR OPIOID USE DISORDER

by
Kaytlyn M. Crowe

Ease of access to prescription opioids and the strength of synthetic opioids have contributed to the rise in over use disorders, overdose, and death rates during the opioid epidemic. The current overdose standard of care, rescue NLX (NLX), is a competitive antagonist to the μ-opioid receptor but has a relatively short period of action compared to opioid agonists, especially synthetic agonists. Rises in the abuse of these synthetic and semi-synthetic agents in recent years have shown the weaknesses of rescue NLX, as it can leave overdose patients vulnerable to renarcotization and precipitated withdrawal. To prevent both from occurring, we developed a slow release, subcutaneous NLX-loaded peptide formulation for the potential management of renarcotization and precipitated withdrawal. We synthesized a series of multidomain peptides with and without loaded NLX and characterized their chemical, mechanical, and biophysical properties. The nanofibrous ultrastructure was assessed with atomic force microscopy (AFM), the secondary structure was probed by Fourier transform infrared spectroscopy in attenuated total reflectance mode (FTIR-ATF), β-sheet formation was confirmed with circular dichroism (CD), and the viscoelastic and thixotropic properties were measured via oscillatory rheometry. *In vitro* cytocompatibility of the peptides was investigated using 3T3 fibroblast cells and a CCK8 assay. To evaluate the long-term release viability of the peptides, an *in vitro* release study was performed for 7 and 30 days.

DRUG RELEASING HYDROGELS FOR OPIOID USE DISORDER

by
Kaytlyn M. Crowe

A Thesis
Submitted to the Faculty of
New Jersey Institute of Technology
in Partial Fulfillment of the Requirements for the Degree of
Master of Science in Biomedical Engineering

Department of Biomedical Engineering
August 2021

APPROVAL PAGE

DRUG RELEASING HYDROGELS FOR OPIOID USE DISORDER

Kaytlyn M. Crowe

Dr. Vivek A. Kumar, Thesis Advisor Associate Professor of Biomedical Engineering, NJIT	Date
Dr. Rajesh Davé, Committee Member Distinguished Professor of Chemical and Materials Engineering, NJIT	Date
Dr. James Haorah, Committee Member Associate Professor of Biomedical Engineering, NJIT	Date

BIOGRAPHICAL SKETCH

Author: Kaytlyn M. Crowe

Degree: Master of Science

Date: August 2021

Undergraduate and Graduate Education:

- Master of Science in Biomedical Engineering,
  New Jersey Institute of Technology, Newark, NJ, 2021

- Bachelor of Science in Biomedical Engineering,
  New Jersey Institute of Technology, Newark, NJ, 2020

Major: Biomedical Engineering

Presentations and Publications:

Crowe, KM, Siddiqui, Z. "Evaluation of Injectable NLX-Releasing Hydrogels." *ACS Applied Bio Materials.* 2020 *3* (11), 7858-7864. DOI: 10.1021/acsabm.0c01016

Panchal, D; Kataria, J; Patel, K; Crowe, KM; et al. "Peptide-Based Inhibitors for SARS-CoV-2 and SARS-CoV." Adv Therapeutics. Accepted.

Adil A, Fiore R, Gannamani S, Griffith A, Hang K, Crowe KM, Kumar VA. "Toothbrush with Onboard Suction and Waste Storage for Evacuation of Aspirates." *Northeast Bioengineering Conference: Undergraduate Research Showcase.* 2021. Abstract and Presentation.

Mom and Dad, I couldn’t have done this without you

ACKNOWLEDGMENT

I would like to thank Dr. Vivek Kumar for his mentorship and guidance these past few years, as well as for serving as my thesis advisor. I would also like to thank Dr. Rajesh Davè and Dr. James Haorah for serving on my thesis committee and for their invaluable comments and suggestions. I would like to acknowledge funding support from NSF 2041092, NIH R15 EY029504, NSF IIP1903617, and NJIT startup funds. I would also like to thank past and present graduate students in the KumarLab: Zain Siddiqui, KaKyung Kim, Abhishek Roy, Joe Dodd-o and Victoria Harbour for their help, friendship, and mentorship. I would like to thank Dr. Amanda Acevado-Jake for mentorship, leadership, and being a great role model for me. I would also like to thank the many undergraduates for their hard work and dedication.

TABLE OF CONTENTS

Chapter	Page
1 INTRODUCTION	1
1.1 Objective	1
2 CHARACTERIZATION OF NLX LOADED PEPTIDES	4
2.1 Solid Phase Peptide Synthesis	4
2.1.1 Synthesis Procedure	4
2.1.2 Hydrogel Formulation and Drug Loading	5
2.2 Chemical and Ultrastructural Characterization	6
2.2.1 Fourier Transform Infrared Spectroscopy	8
2.2.2 Circular Dichroism	8
2.2.3 Atomic Force Microscopy	10
2.3 Mechanical Characterization	12
3 *IN VITRO* CYTOCOMPATIBILITY AND RELEASE	15
3.1 *In Vitro* Cytocompatibility	15
3.2 *In Vitro* Release Profile	18
4 CONCLUSION AND FUTURE STEPS	22
4.1 Conclusion	22
4.2 Next Steps	22
APPENDIX	24
REFERENCES	25

LIST OF TABLES

Table		Page
2.1	Sequences and Properties of ASPs ……...……..…….	6

LIST OF FIGURES

Figure		Page
1.1	Design of amphiphilic self-assembling peptides (ASP) for release of NLX. ……	3
2.1	Fourier transform infrared (FTIR) fingerprint spectra. ……..……	7
2.2	Circular dichroism (CD) of peptide hydrogels. ……..……	9
2.3	Atomic force microscopy (AFM) of diluted peptide hydrogels. ...…….	11
2.4	Oscillatory shear thinning of peptide hydrogels. ...……	13
2.5	Thixotropic shear recovery of peptide hydrogels. ……..……...	14
3.1	Cytocompatibility assay of peptide hydrogels. ……..……	17
3.2	Seven day release of NLX from peptide hydrogels. ……..	20
3.3	Thirty day release of NLX from peptide hydrogels. ……..	21
A.1	Mass spectroscopy of K_2 and E_2. ...…….	24

LIST OF SYMBOLS

β	Beta
μ	Mu
NLX	NLX
NTX	Naltrexone
K_2	Positively charged, Lysine functionalized self assembling peptide
E_2	Positively charged, Glutamic Acid functionalized self assembling peptide
w%	Weight percent
~	Approximately

LIST OF DEFINTIONS

NLX	Opioid antagonist- used to reverse opioid overdose
Naltrexone	Opioid antagonist- used in opioid abuse rehabilitation

CHAPTER 1

INTRODUCTION

1.1 Objective

The μ-opioid receptor antagonist NLX (NLX) is the current gold-standard for opioid overdose rescue[1-4]. However, NLX has a short half-life around 75 minutes[5], and rescue does must be administered several times to prevent a patient from going back into a state of overdose, a phenomenon known as renarcotization[6, 7]. Overdoses caused by synthetic opioids present a more significant risk of renarcotization[1], and patients who are taken to a hospital are put on intravenous NLX for 6 to 8 hours to prevent renarcotization[5]. Unfortunately, there is a significant portion of opioid users[8, 9] who do not enter hospital care after receiving the first dose of NLX, leaving them wide open for renarcotization and death from an overdose that could have been stopped[2, 10, 11]. This presents a gap in which long-acting NLX formulations are needed to provide acute rescue benefit, reduce the potential of renarcotization and, if tuned appropriately, potentially mitigate precipitated withdrawal. The central hypothesis is that release of NLX can be controlled from implantable subcutaneous self-assembling amphiphilic peptide hydrogel[12-16] reservoirs that promote prolonged NLX stability (Figure 1.1 A, B). These amphiphilic self-assembling peptides (ASPs) can sequester partially lipophilic/ hydrophobic drugs[12, 15, 17-19] such as NLX and can be formulated into thixotropic hydrogels in aqueous buffers at physiological pH and ionic strength[13-17, 20]. The objectives were the following: (a) to synthesize a series of ASPs and characterize their biomechanical properties, (b) determine the *in vitro* cytocompatibility, and (c) determine an *in vitro* release profile.

Ultimately, the goal is to be able to provide an injectable depot that can be administered in clinics or after rescue NLX is used, in situations when patients are at most risk for renarcotization (Figure 1.1 B, C, D). A longer term goal is also to provide a bridge between the event of an overdose occurring and when a patient can begin rehabilitation treatment.

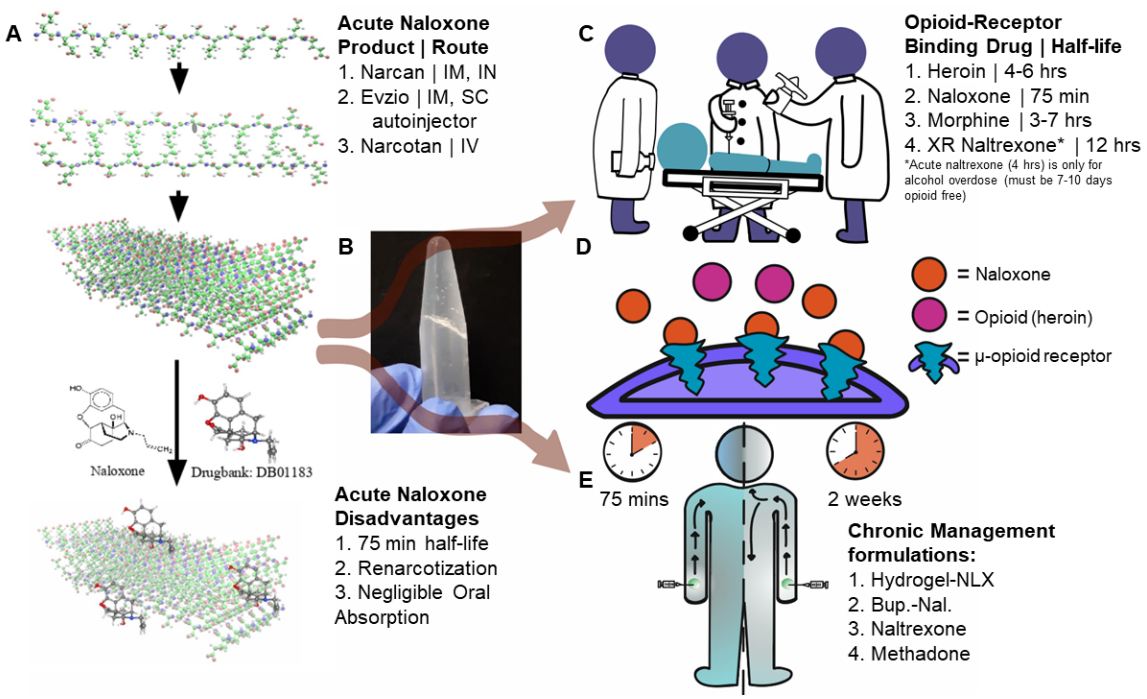

Figure 1.1 Design of amphiphilic self-assembling peptides (ASP) for release of NLX. (A) Noncovalent interactions initiate the self-assembly mechanism. Alternating hydrophilic serine and hydrophobic leucine residues form hydrogen bonds, and assemble into dimers, tetramers, nanofibers, and further form antiparallel β-sheet fibers. Drugs or other small molecules can be added to the ASPs because of the aqueous (sucrose or phosphate buffer) composition of the gel (B). (C) NLX can be dosed intramuscularly (IM), intranasally (NAS), subcutaneously (SC), or intravenously (IV), but has a relatively short half-life, especially when compared to other opioid type drugs. (D) NLX is a high affinity μ-opioid antagonist, and preferentially binds to the receptor over agonists such as heroin. (E) For prevention of renarcotization and more chronic opioid management, a 2-week continuous release of NLX is considered.

CHAPTER 2

CHARACTERIZATION OF NLX LOADED PEPTIDES

2.1 Solid Phase Peptide Synthesis

A peptide is a short chain of individual amino acid residues linked by peptides bonds, where the carboxyl group (-CO_2H) of one amino acid is bound to the amino group (-NH_2) of the next residue. The twenty common amino acids have side chain functional groups (-R) that can have a negative, positive, or neutral electric charge, polarity, or other attributes that will carry over into the peptide that is created[21]. The overall charge of peptides, as well as local charge distribution, can drastically alter the solubility of peptides, as well as their biological activity[21]. While NLX has no net formal charge at pH 7, K_2 is positively charged and E_2 is negatively charged. Two oppositely charged ASPs were chosen to see if the charge of the scaffold had a difference on the release of NLX from the ASP scaffolds.

2.1.1 Synthesis Procedure

Solid phase peptide synthesis (SPPS) is the method of choice for most peptide synthesis today[22]. SPPS has advantages over both liquid phase peptide synthesis and recombinant peptide synthesis in that it allows the user increased control over the physical and electrochemical properties of the peptide in question, the process is now automated with a relatively short production cycle, and allows for the rapid synthesis of medium chain peptides[22, 23] (<50 amino acids). However, as with all peptide synthesis methods, the raw materials are expensive, and the purification process for SPPS products can be complex and lengthy. Fmoc (9-fluorenylmethoxycarbonyl) group is used as a protecting group on

alpha amino groups in most amino acids that will be used for SPPS[22]. The alpha amino group needs protecting to prevent oxidation and premature reaction of the amino acid during storage[22]. While there are other protecting groups, Fmoc is popular as the primary protecting agent because it limits contact with trifluoroacetic acid (TFA), a strong organic acid, during the actual synthesis[22]. SPPS occurs in stages, starting with an insoluble resin bead. The resin bead is an anchor for the peptide as it is built, holding on to the C-terminus. There are different types of resins for different peptide chemistries, including Brominated Wang resin for Boc SPPS and Rink amide resin for Fmoc SPPS. After anchoring the resin bead, the next stage is deprotection of the amino acid and removal of Fmoc via a strong base: piperidine or piperizine[22]. Once deprotection has occurred, coupling between amino acids is done using a combination of activators (Oxyma and DIC/DCC) in a neutral environment. The process of steps is repeated until the peptide chain is complete and the N-terminus is acetylated[22]. The peptide must now be cleaved from the resin bead. To do this, a cleavage cocktail of TFA, TIS, DoDT, and MilliQ H_2O is prepared and added to the peptide to remove the peptide from the resin, as well as the side chain protecting groups. The cleavage cocktail is important because while the TFA is doing the main work of cleaving the peptide from the resin, the TIS and H_2O are ion scavengers, and the DoDT prevents oxidation and side reactions from the Boc/t-butyl protected side groups that are no longer protected. After cleaving, the TFA cocktail must be washed out of the peptide with ether and dried, and the final peptide is obtained via dialysis and lyophilization[22].

2.1.2 Hydrogel Formulation and Drug Loading

Previously published work from our group[12-16, 20, 24-28] and others[18, 19, 29, 30] has shown the

ability of an alternating (-S) serine (hydrophilic) and (-L) leucine (hydrophobic) amino acid backbone to self-assemble into anti-parallel β-sheet nanofibers (Figure 1.1 A). We synthesized two amphiphilic self-assembling peptides (ASPs) as shown in Table 2.1 below with SPPS. The mass spectra of the synthesized peptides are shown in Figure A.1. We hypothesized that the charged matrices of the ASPs could modulate the prolonged release of NLX.

Table 2.1 Sequences and Properties of ASPs

Peptide	Charge	Sequence	Form	Secondary Structure
K_2	Positive	$K_2(SL)_6K_2$	Hydrogel	β-sheet
E_2	Negative	$E_2(SL)_6E_2$	Hydrogel	β-sheet

After lyophilization, 20 mg of each ASP was dissolved in 1 ml of 298 mM sucrose, pH adjusted to 7, to formulate 2 weight percent (2 w%) hydrogels[12, 14, 15]. In order to mix NLX into the hydrogels, NLX hydrochloride was dissolved in 298 mM sucrose to reach 2 w% prior to combining with the hydrogels[12-15, 31]. An equivalent volume of each 2 w% NLX solution and 2 w% hydrogel were mixed to give 1 w% of K_2NLX and E_2NLX. Similarly, lower concentrations of NLX hydrochloride were prepared and mixed with hydrogels in a 1:1 ratio for release experiments described in chapter 3.

2.2 Chemical and Ultrastructural Characterization

The secondary structure of proteins and peptides can be identified with Fourier Transform Infrared Spectroscopy (FTIR) and Circular Dichroism (CD). FTIR uses the unique vibration frequencies of bond types to identify them, as well as secondary

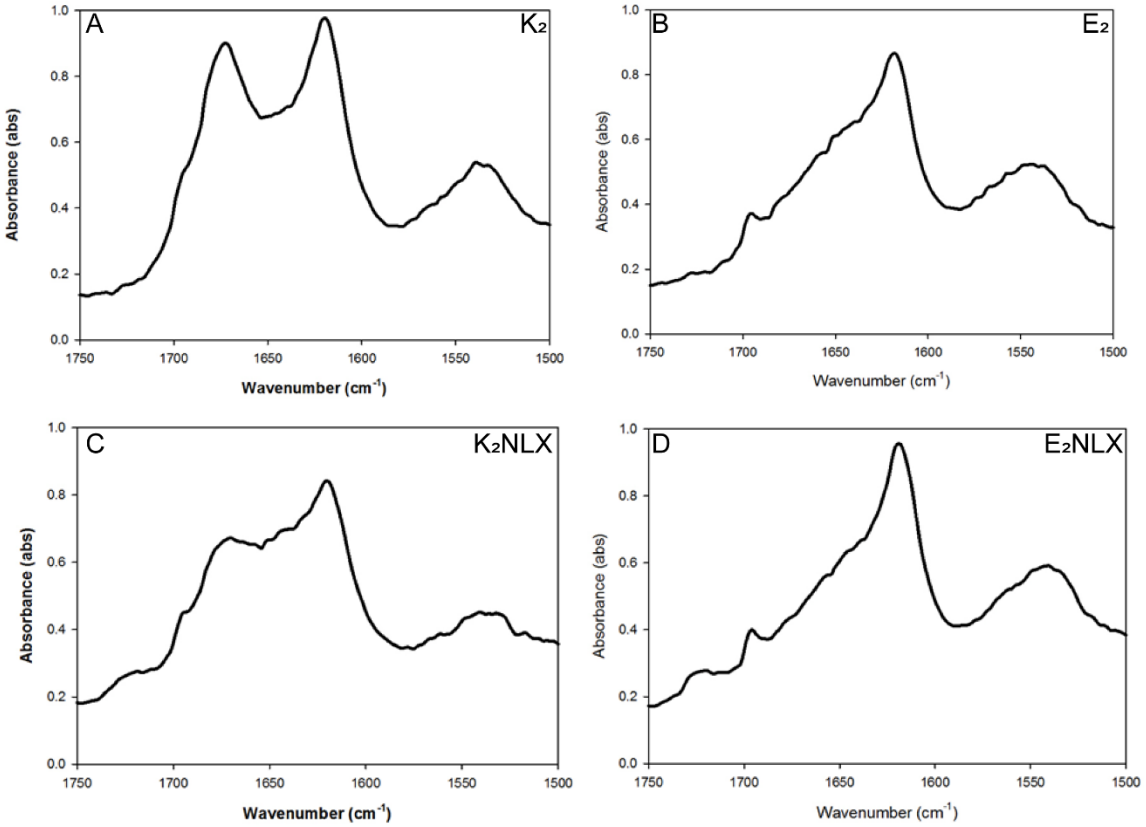

Figure 2.1 Fourier transform infrared (FTIR) fingerprint spectra. All (A-D) display a characteristic β-sheet amide I peak around 1622 cm^{-1} and lysine side shoulders around 1673 cm^{-1}.

structures such as α-helices and β-sheets. CD uses light to identify secondary protein structures based on the polarization of light from the chiral molecules within the sample. Surface structure and nanofiber quality is assessed by Atomic Force Microscopy (AFM), which provides information about the height and width of the individual fibers[21, 32].

2.2.1 Fourier Transform Infrared Spectroscopy

FTIR attenuated total reflectance (FTIR-ATR) mode was used to probe the secondary structure of the peptide hydrogels. Samples were prepared as in 2.1.2 and diluted in MilliQ water to 0.1 mg/mL. Aqueous samples were mounted onto a cleaned potassium bromide (KBr) plate on a Perkin-Elmer IR spectrophotometer 100 for spectral analysis between 400-4000 cm^{-1}, after scanning a pure MilliQ water background[12-15, 17, 31]. K_2, E_2, K_2NLX, and E_2NLX were all observed (Figure 2.1) with characteristic peaks for β-sheet specific amide I peaks at ~1620 cm^{-1}, which confirms the amphiphilic assembly of the $(SL)_6$ backbone[12-15, 17, 31]. There is a shoulder at ~1670 cm^{-1} that represents the lysine sides, though this could also be trace remnants of trifluoroacetate from peptide synthesis.

2.2.2 Circular Dichroism

Circular dichroism (CD) experiments were performed on a Jasco J-810 spectropolarimeter to determine the initial β-sheet secondary structure, and to ensure its preservation after the addition of NLX. Experiments were conducted at room temperature in a 1 m cuvette. Formulations were prepared as in 2.1.2 and diluted in MilliQ water to a concentration of 0.1 mg/mL and scanned from 190-260 nm (Figure 2.2). Molar residual ellipticity was then calculated and compared to references for secondary structure (α-helix and β-sheet)[24]. The minimum trough at ~215 nm and peak at ~195 nm for K_2, E_2, K_2NLX, and E_2NLX, indicate the presence of β-sheet

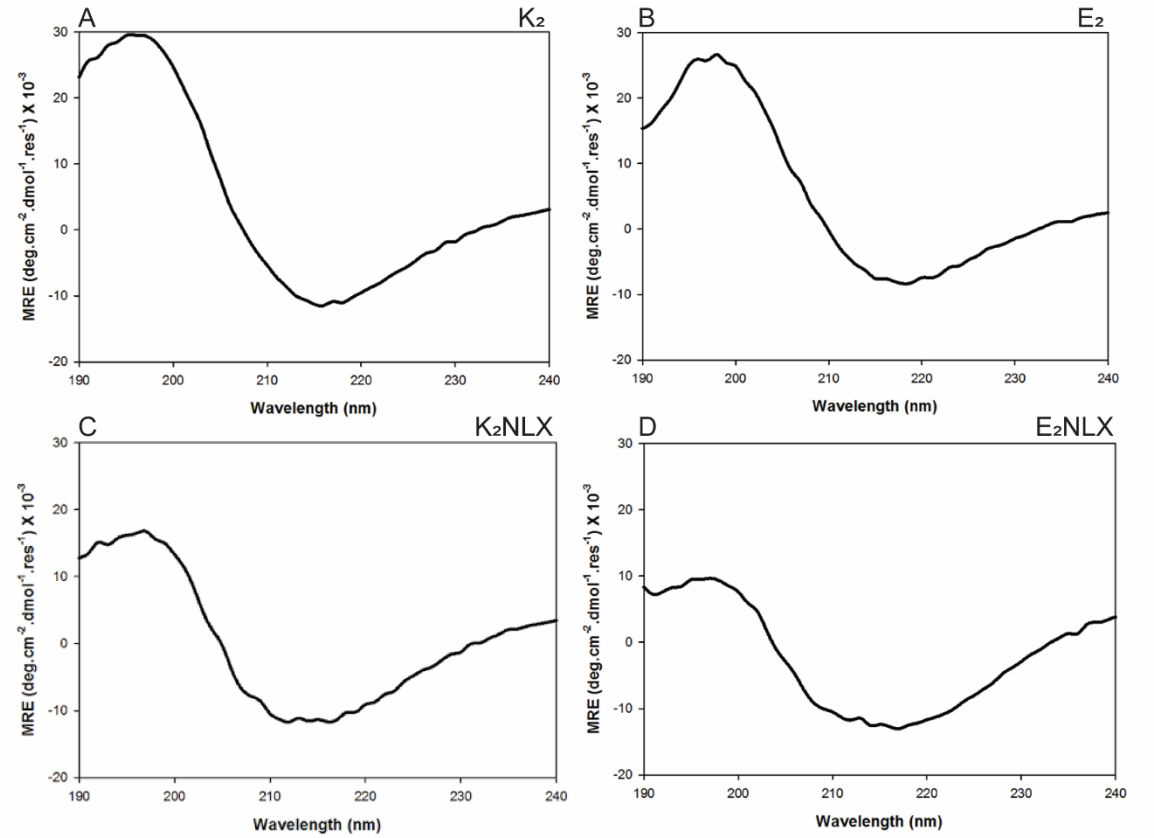

Figure 2.2 Circular dichroism (CD) of peptide hydrogels. All (A-D) show β-sheet characteristic troughs around 215 nm and maxima around 195 nm, indicating that the addition of NLX does not significantly alter the formation of the β-sheet secondary structure.

secondary structures within the peptide, undisturbed by the addition of NLX.

2.2.3 Atomic Force Microscopy

Atomic force microscopy (AFM) was performed to confirm peptide strand morphology and measure nanofiber height and width. Hydrogel samples of K_2, E_2, K_2NLX, and E_2NLX were prepared as in 2.1.2 and diluted in MilliQ water to a concentration of 0.1 mg/mL. The diluted peptide was spin-coated on a freshly cleaved mica disk. After spin-coating, the sample was washed with DI water twice and dried overnight. Imaging performed using ScanAsyst mode on a Dimension Icon instrument was used to observe the prepared sample (Figure 2.3). The average width of K_2NLX is 10.6 ± 1.6 nm, which is consistent with the width of K_2 (10.6 ± 2.7 nm). E_2NLX similarly showed 8.7 ± 0.9 nm, which is consistent with the width of E_2 (8.9 ± 1.2 nm)[30].

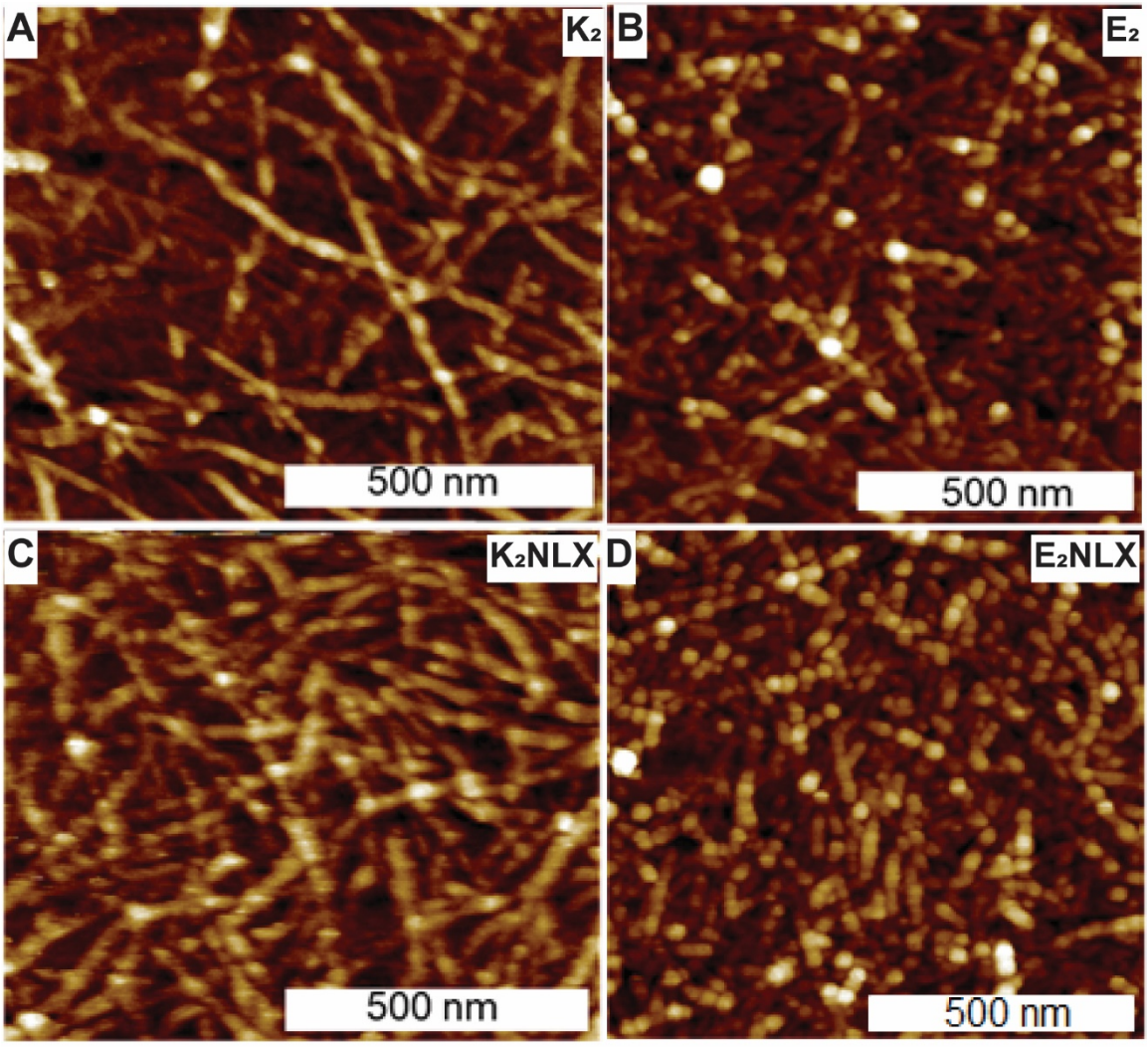

Figure 2.3 Atomic force microscopy (AFM) of diluted peptide hydrogels. All (A-D) show individual fiber formation, showing consistent width and height (1.3-1.6 nm) despite the addition of NLX (C, D).

2.3 Mechanical Characterization

The peptide hydrogels that were synthesized for this work, and are generally the focus of our group, are soft gels with relatively low tensile strength[14, 20, 24]. They are meant to be injected or sprayed, similar in delivery to the current delivery mechanisms of NLX today. In order to accurately measure the viscoelastic properties of the hydrogels, oscillatory rheometry is performed to determine the storage and loss moduli. To be sure that the hydrogels are injectable, we also perform strain sweep and shear recovery tests to measure thixotropic properties.

Oscillatory rheometry was performed with a 4 mm plate geometry placed as an upper plate and 40 μL of the prepared hydrogel loaded onto the bottom plate at a gap length of 250 μm (n = 4). To perform the strain sweep (Figure 2.5), the loaded hydrogel was prestrained at a constant 1% strain and a frequency of 1 Hz for 5 min and followed by an increase in strain from 0.1 to 100% strain for 5 min. K_2 and K_2NLX showed liquefaction at higher strains than E_2 and E_2NLX (~70% vs. ~ 30%), but all showed inversion of G' and G". The addition of NLX did not affect the elastic moduli of the hydrogels, and they exhibited similar stiffness (Figure 2.5).

For the shear recovery test (2.6) the upper plate oscillated between periods of 1% strain for 120 s and 100% strain for 60 s, again at 1 Hz for 5 min. All four peptide hydrogels exhibited rapid recovery of bonds in a repeatable manner when under cyclic shear strains. The repeated shearing cycles did not cause an interruption in the storage modulus or the rapid gelation under low-strain (>95% G' recovery within 5 s) (Figure 2.6).

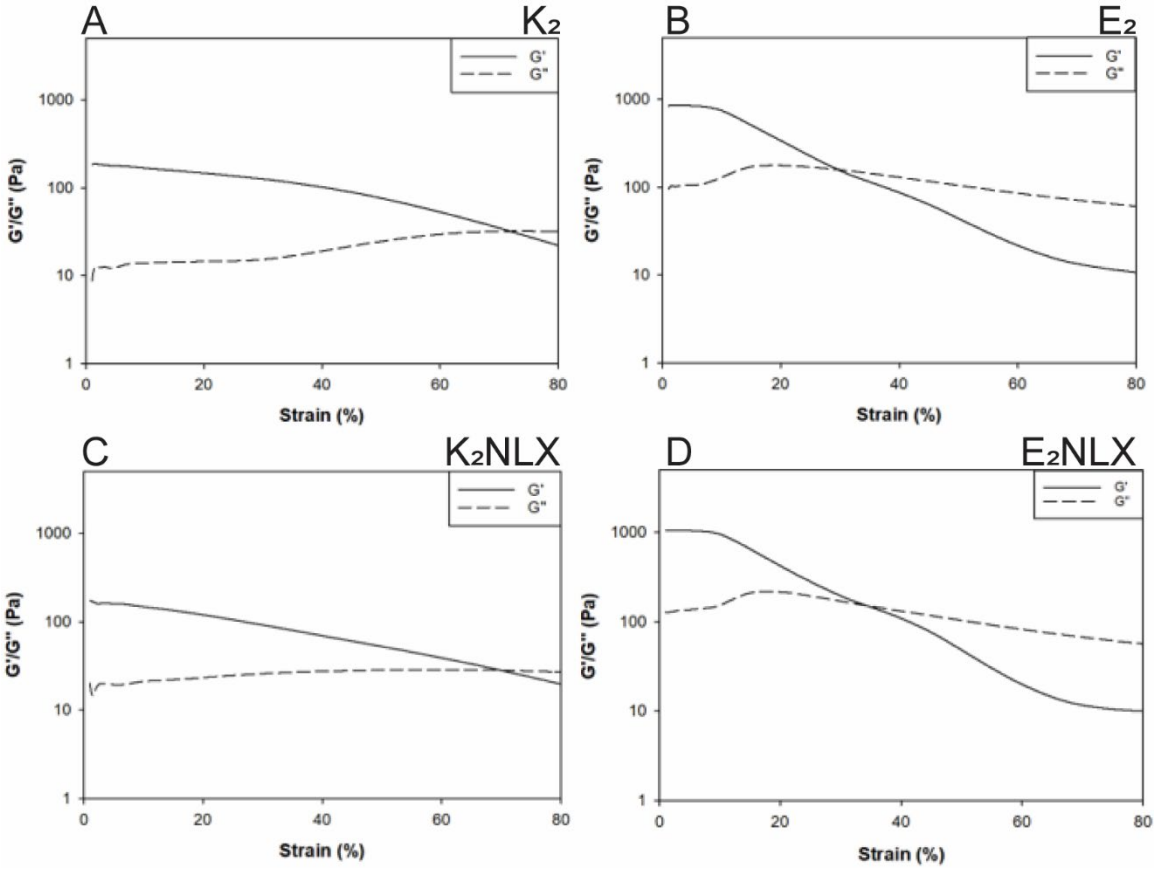

Figure 2.4 Oscillatory shear thinning of peptide hydrogels. All (A-D) show syringe injectability. The low strain, the elastic modulus, G', remains higher than the viscous modulus, G". However, at high strain, G' and G" show inversion and illustrate liquefaction of the hydrogel.

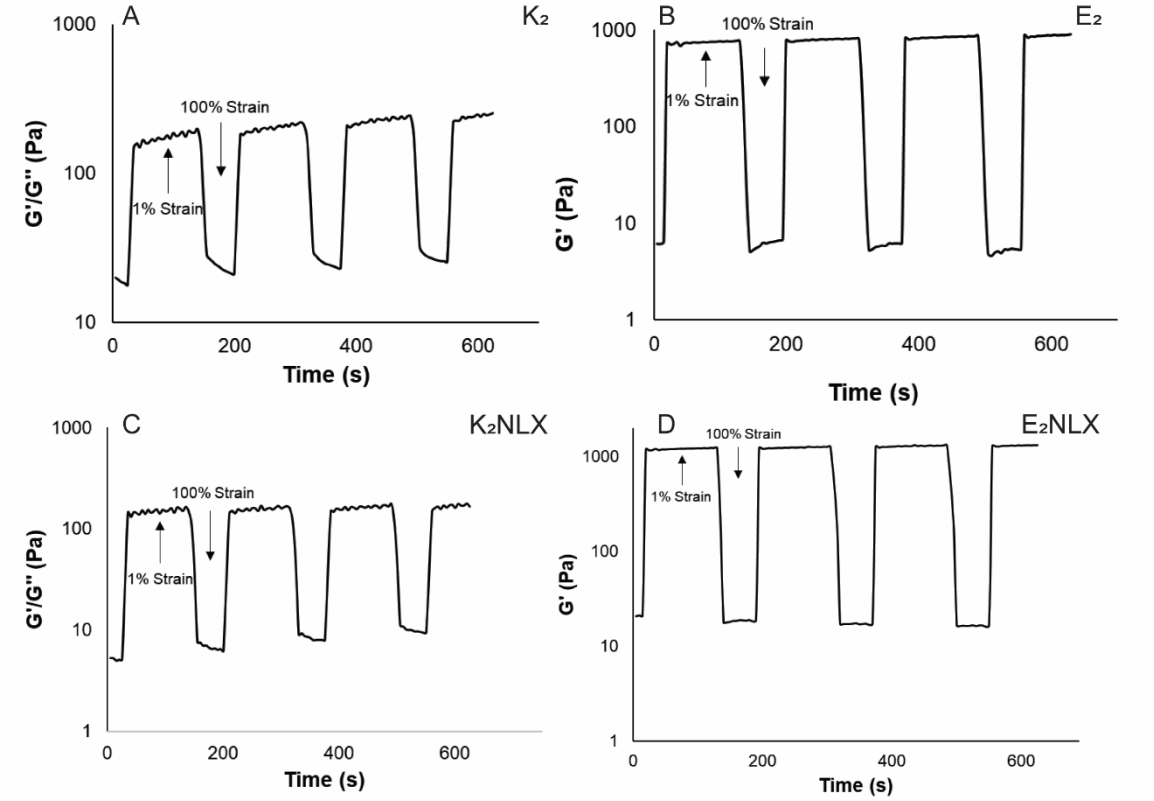

Figure 2.5 Thixotropic shear recovery of peptide hydrogels. All (A-D) exhibit liquefaction at 100% strain, but recover rapidly into hydrogels (high G') after removal of strain. Minimal hysteresis noted after repeated cyclic shearing (100% strain, 60 s; 1% strain, 120 s).

CHAPTER 3

IN VITRO CYTOCOMPATIBILITY AND RELEASE

3.1 *In Vitro* Cytocompatibility

In order to assess the overall cytocompatibility of the peptides (K_2, E_2, K_2NLX, and E_2NLX), we ran an *in vitro* CCK8 cytocompatibility assay with 3T3 fibroblasts. The CCK8 assay is a sensitive colorimetric assay that uses the highly water-soluble tetrazolium salt WST-8 to measure the dehydrogenase activity in cells. The dehydrogenase activity generates orange formazan dye from WST-8, which is directly proportional to the number of living cells and so can be used for measuring the cytotoxicity of various conditions. As such, the following peptide weight percentages: 0.1 w%, 0.01w%, 0.001w% (Figure 3.1) were used in the assay. 3T3 fibroblasts were cultured following previous protocol and seeded after the first passage from frozen. After the first passage, fibroblasts were seeded at a cell density of 10,000 cells per well in a 96-well plate (n = 5) in complete fibroblast media (90% DMEM, 10% FBS, and 1% Pen-Strep) for 24 h in an incubator maintained at 37 °C and 5% CO_2[24]. The fibroblast media was aspirated, and the peptide conditions (3 w% conditions x 4 peptide types) prepared in serum-free media were delivered to all but control (serum-free media) wells. The peptide conditions and controls were incubated for 6 hrs. After aspirating the samples, the wells were washed with 200 µL of PBS, and 100 µL of PBS was added to each of the wells along with 10 µL of CCK8 stain[24]. After 1 h of incubation, we used a TECAN M200 Infinite plate reader to analyze the 96-well plate at an absorbance of 450 nm against a reference wavelength of 650 nm[24] as per manufacturer instructions. The results were

analyzed with ANOVA and normalized to the media-only control (Figure 3.1).

Higher levels of cell proliferation occurred when there were higher levels of peptide hydrogel, as the hydrogel matric mimics the ECM. Quantitatively, E_2(0.1 w%) by itself had the highest absorbance (and lowest cytotoxicity), but this is not statistically significant compared to the media-only controls as the ANOVA values overlap.

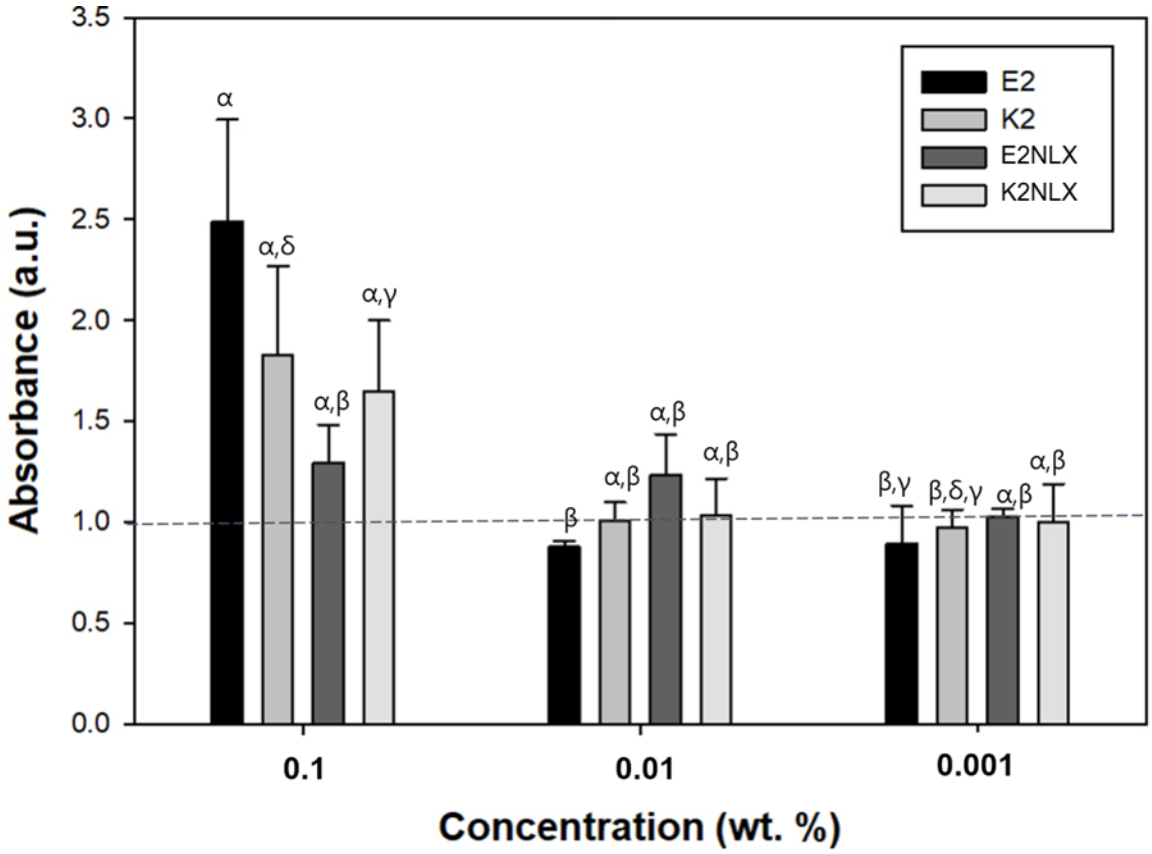

Figure 3.1 Cytocompatibility assay of peptide hydrogels. No conditions exhibited cytotoxicity relative to each other. Cell proliferation occurred at higher ECM-mimetic hydrogel concentration levels. Analysis was performed via ANOVA, with similar Greek letters indicating no statistically significant difference in absorption ($p < 0.05$).

3.2 *In Vitro* Release

To measure the release of NLX from hydrogels, a colorimetric release assay was utilized. K_2 and E_2 hydrogels (1 wt %) were loaded with 10 mg/mL or 1 mg/mL NLX hydrochloride for a total of four groups. Each group was tested over two time periods. Two hundred microliters of each NLX hydrogel was added to a microcentrifuge tube and covered with 1 mL of 1× PBS (n = 4 per time point)[26]. Release experiments took place over 30 days in an incubator maintained at 37 °C, 100% humidity, and 5% CO_2[26]. NLX release was measured at time points: 1, 2, 4, 8, and 24 h and 2, 3, 4, 5, 6, 7, 9, 11, 13, 15, 18, 21, 24, 27, and 30 days (Figure 3.2, 3.3). At each time point, the full 1 mL of 1× PBS was removed from the microcentrifuge tube for NLX release analysis and replaced with 1 mL of fresh 1× PBS[26, 30]. Release was quantified by measuring NLX absorbance at 230 nm and comparing to a NLX standard curve from 0.001 to 1.4 mg/mL using a NanoQuant on a Tecan M200 Infinite Pro microplate reader[26, 30]. Reported uptake at each time point is the average of at least two independent measurements from a total of four independent release experiments.

NLX released from K_2 and E_2 hydrogels was normalized to the total NLX loaded into the hydrogel, expressed as M/M_{inf}[26, 30]. The release curves were fit against several using SigmaPlot's custom curve fit library, "release.jfl," for drug release. The model with the best fit (R^2 value closest to 1) was selected to predict the release. Weibull (majority) and Korsmeyer−Peppas (1 mg/mL E_2NLX) models best predicted all data sets; for all release curves analyzed ($R^2 > 0.97$) (Figure 3.2, 3.3). The experimentally observed release (points) was plotted with the release predicted by the model (solid line) and 95% prediction bands (dashed lines).

There was successful release of NLX from the seven day hydrogels and the thirty day hydrogels. In the thirty day study, the 1 mg/mL gels did significantly better than the 10 mg/mL get, releasing above 80% around day 5, whereas the 10 mg/mL gels never got reached 80%. After day 5, K_2NLX(1 mg/mL) kept increasing slightly while E_2NLX(1 mg/mL) was decreasing. However, both are well within the 95% prediction bands. The seven day study again produces good release of NLX for the 1 mg/mL (above 90% by day 4), and the 10 mg/mL group reaches the underside of 80% by the end of the study, which is comparable to what was achieved in the thirty day study group.

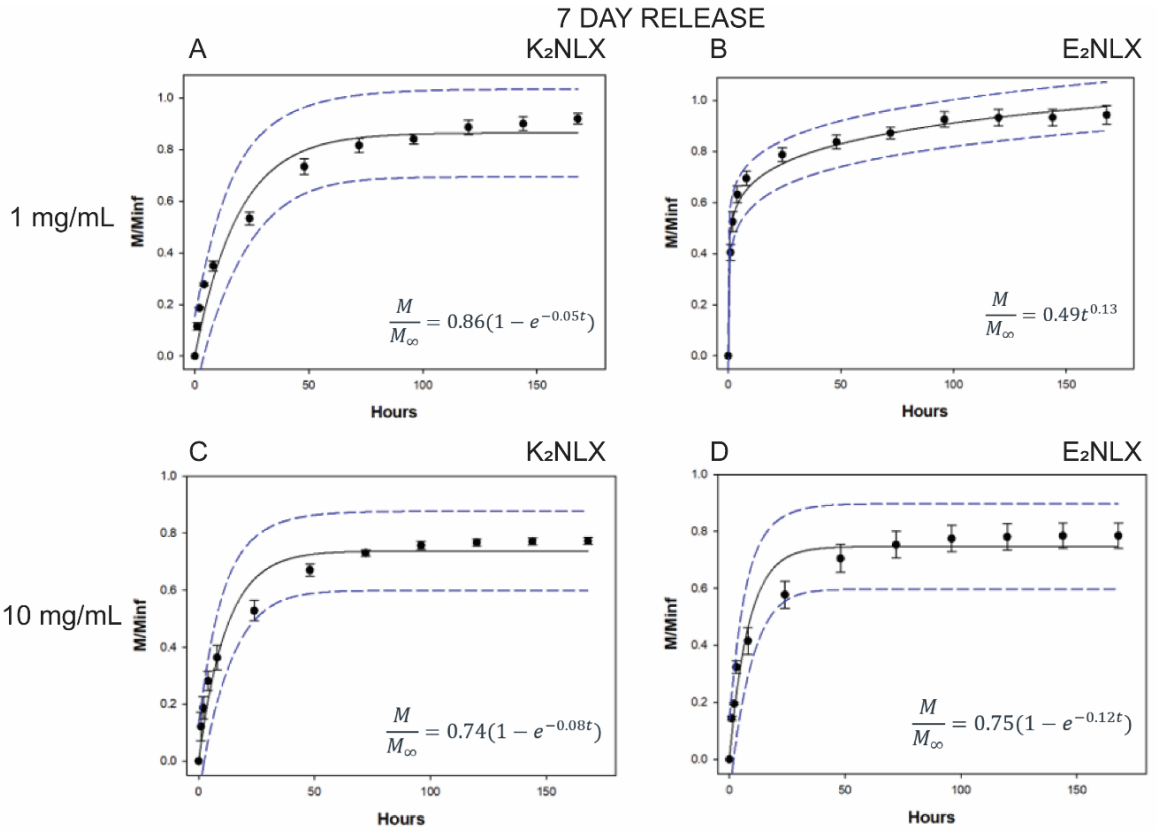

Figure 3.2 Seven day release of NLX from peptide hydrogels. (A) K_2NLX and (B) E_2NLX gels with 1 mg/mL NLX loading showed ~80% release between 4-7 days. (C) K_2NLX and (D) E_2NLX gels with 10 mg/mL NLX loading showed ~80% release by 3-4 days. The release was modeled on a solid line ($R^2 > 0.97$ for all plots) and 95% prediction bands (dashed lines).

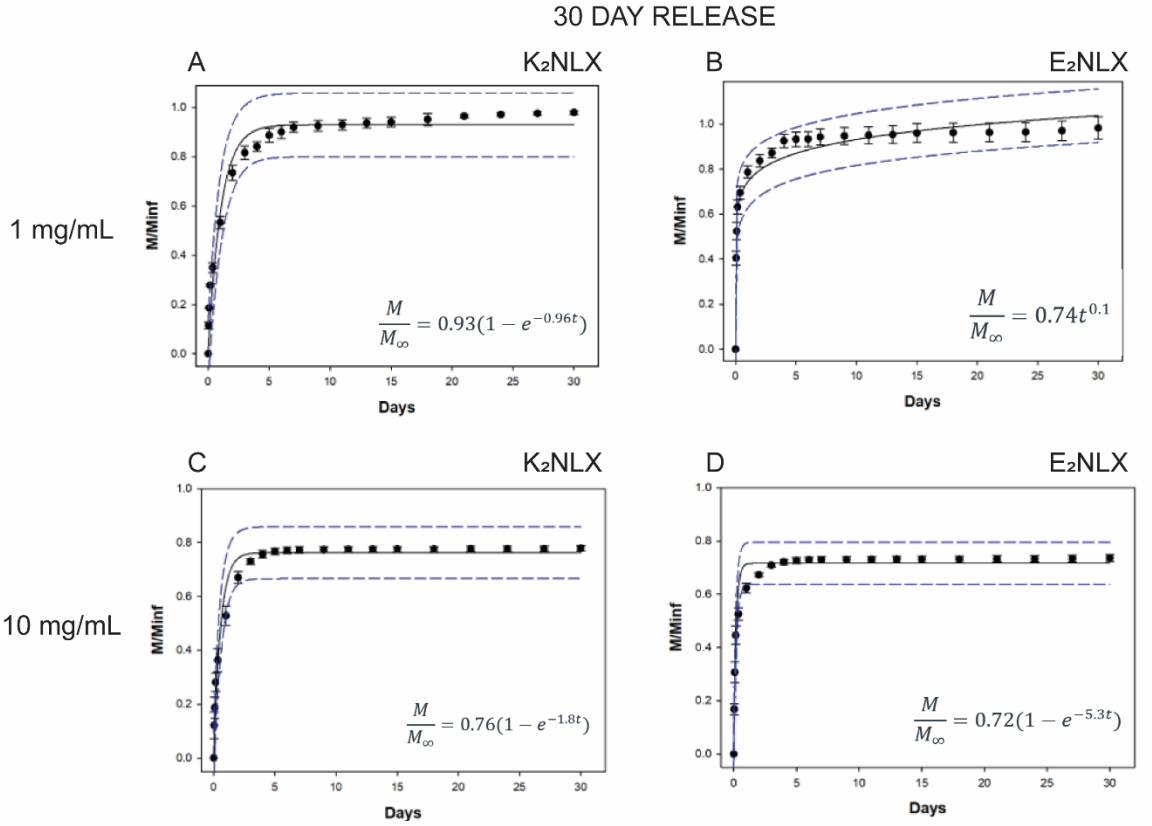

Figure 3.3 Thirty day release of NLX from peptide hydrogels. (A) K_2NLX and (B) E_2NLX gels with 1 mg/mL NLX loading showed ~80% release by 5 days, and continued to release for the remainder of the study. (C) K_2NLX and (D) E_2NLX gels with 10 mg/mL NLX loading showed slightly less than 80% release at 5 days, and continued releasing consistently. The release was modeled on a solid line ($R^2 > 0.97$ for all plots) and 95% prediction bands (dashed lines).

CHAPTER 4

CONCLUSION AND FUTURE STEPS

4.1 Conclusion

Self assembling peptide hydrogels provide a novel scaffold for the release of small molecule drugs. The ability to alter the mechanical properties of the gel to make it accessible to different populations in need is especially important when considering an application like releasing NLX, as many people might not have the training needed for safe injections. The synthesized ASP peptide hydrogels are mechanically robust, β-sheet forming hydrogels that can be loaded with NLX without changing the inherent properties of the hydrogel. Our hypothesis that the hydrogel can modulate the release of NLX over time is supported by our findings. We demonstrate that NLX can be loaded into multiple hydrogel formulations at multiple concentrations and be released over a period of days at high efficiency. The intact biomechanical properties of the hydrogel scaffold is important implication in delivery of NLX, with shear stress from a needle causing liquefaction when injected, but the bolus remaining in place for several days as the medication is delivered.

4.2 Future Steps

The future steps for the NLX loaded hydrogels include pharmacokinetic (PK) and pharmacodynamic (PD) testing, and *in vivo* models. To further understand the mechanism of how the NLX is releasing from the hydrogel scaffold, we would run plasma PK and PD testing. Hydrogels loaded with varying concentration of NLX, along with pure NLX would be injected into naïve rats, and plasma would be extracted over a

period of hours and days in order to measure the degradation rate and *in vivo* metabolism. Another future step would be done in collaboration with Dr. Benedict Kolber and his group at the University of Pittsburgh. There, opioid models of analgesia can be performed. We would send them loaded hydrogel and naïve rats would be injected in the back on day 0. On testing days, they would get doses of an opioid near the same spot as the hydrogel bolus. A von Frey filament test will be performed. During the test, a small filament is pressed to the hind paw until the animal flinches, moves away, or some other aversive behavior is notices.

Other potential avenues of work are adding buprenorphine to the scaffold in addition to NLX, to create a rehabilitation medication that cannot be abused. We could also dispense opioids for pain relief after surgery instead of doctors having to prescribe opioids with the potential for abuse, which could then lead to the need for NLX.

APPENDIX A

MASS SPECTROSCOPY

Figure A.1 shows the mass spectroscopy of K_2 and E_2.

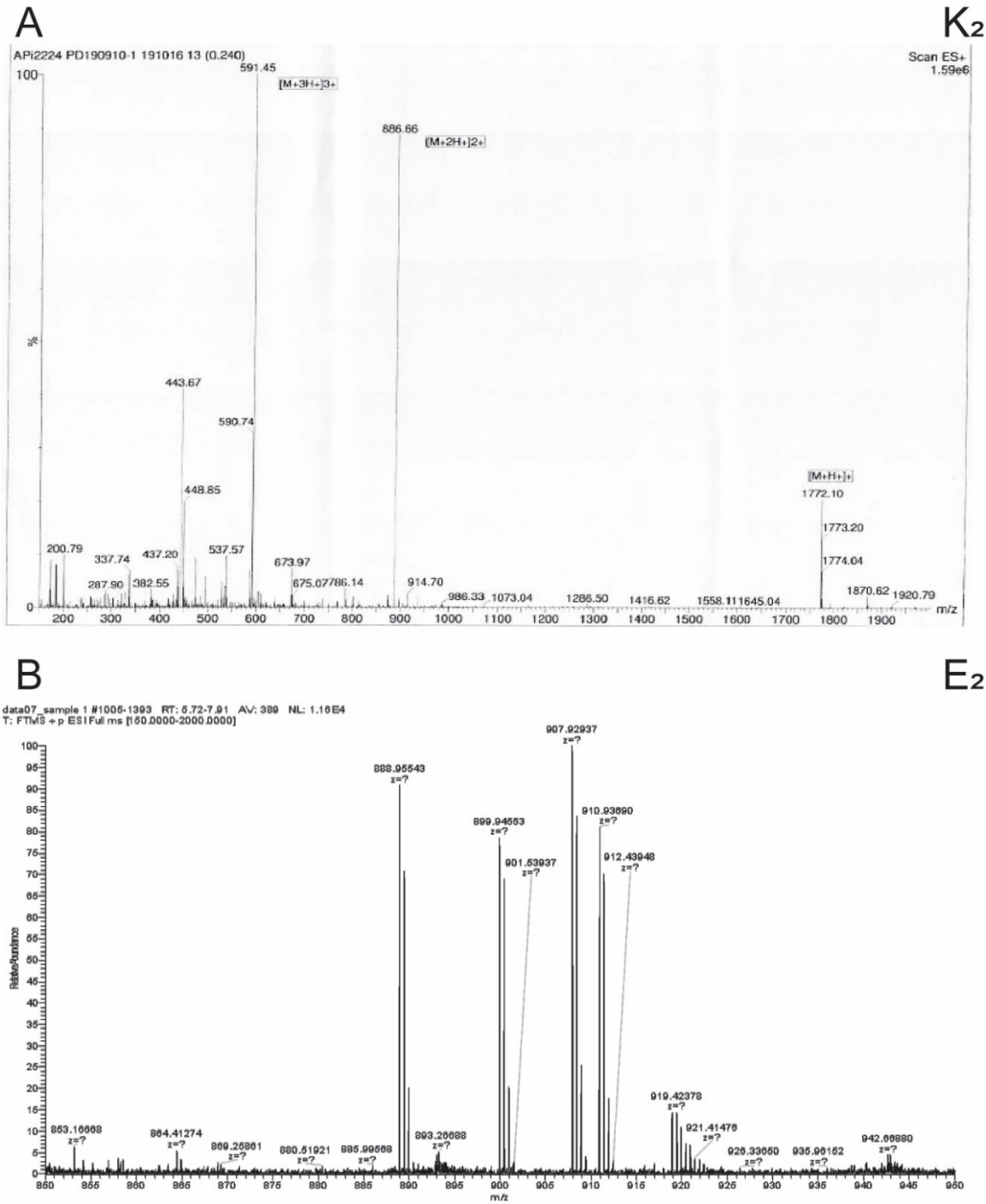

Figure A.1 Mass Spectroscopy of K_2 and E_2.

REFERENCES

1. Rzasa Lynn, R.; Galinkin, J. L., NLX dosage for opioid reversal: current evidence and clinical implications. *Ther Adv Drug Saf* **2018,** *9* (1), 63-88.
2. Hedegaard, H. M., Arialdi M; Warner, Margaret, Drug Overdose Deaths in the United States, 1999-2018 Key findings Data from the National Vital Statistics System, Mortality. Services, U. D. o. H. a. H., Ed. CDC, National Center for Health Statistics: 2020; Vol. 356.
3. Barnett, V.; Twycross, R.; Mihalyo, M.; Wilcock, A., Opioid Antagonists. *Journal of Pain and Symptom Management* **2014,** *47* (2), 341-352.
4. Algera, M. H.; Kamp, J.; van der Schrier, R.; van Velzen, M.; Niesters, M.; Aarts, L.; Dahan, A.; Olofsen, E., Opioid-induced respiratory depression in humans: a review of pharmacokinetic-pharmacodynamic modelling of reversal. *Br J Anaesth* **2019,** *122* (6), e168-e179.
5. Wanger, K.; Brough, L.; Macmillan, I.; Goulding, J.; MacPhail, I.; Christenson, J. M., Intravenous vs subcutaneous NLX for out-of-hospital management of presumed opioid overdose. *Acad Emerg Med* **1998,** *5* (4), 293-9.
6. Kassick, A. J.; Allen, H. N.; Yerneni, S. S.; Pary, F.; Kovaliov, M.; Cheng, C.; Pravetoni, M.; Tomycz, N. D.; Whiting, D. M.; Nelson, T. L.; Feasel, M.; Campbell, P. G.; Kolber, B.; Averick, S., Covalent Poly(lactic acid) Nanoparticles for the Sustained Delivery of NLX. *ACS Appl Bio Mater* **2019,** *2* (8), 3418-3428.
7. Lewter, L. A.; Johnson, M. C.; Treat, A. C.; Kassick, A. J.; Averick, S.; Kolber, B. J., Slow-sustained delivery of NLX reduces typical NLX-induced precipitated opioid withdrawal effects in male morphine-dependent mice. *J Neurosci Res* **2020**.
8. Haffajee, R. L.; Lin, L. A.; Bohnert, A. S. B.; Goldstick, J. E., Characteristics of US Counties With High Opioid Overdose Mortality and Low Capacity to Deliver Medications for Opioid Use Disorder. *JAMA Netw Open* **2019,** *2* (6), e196373.
9. Kiang, M. V.; Basu, S.; Chen, J.; Alexander, M. J., Assessment of Changes in the Geographical Distribution of Opioid-Related Mortality Across the United States by Opioid Type, 1999-2016. *JAMA Netw Open* **2019,** *2* (2), e190040.
10. H., H.; Bastian, B. S.; Trinidad, J. P.; Spencer, M.; Warner, M., *Drugs most frequently involved in drug overdose deaths: United States, 2011-2016*. US Department of Heath and Human Services: 2018; Vol. 67.
11. Scholl, L.; Seth, P.; Kariisa, M.; Wilson, N.; Baldwin, G., Drug and Opioid-Involved Overdose Deaths - United States, 2013-2017. *MMWR Morb Mortal Wkly Rep* **2018,** *67* (5152), 1419-1427.
12. Kumar, V. A.; Liu, Q.; Wickremasinghe, N. C.; Shi, S.; Cornwright, T. T.; Deng, Y.; Azares, A.; Moore, A. N.; Acevedo-Jake, A. M.; Agudo, N. R.; Pan, S.; Woodside, D. G.; Vanderslice, P.; Willerson, J. T.; Dixon, R. A.; Hartgerink, J. D., Treatment of hind limb ischemia using angiogenic peptide nanofibers. *Biomaterials* **2016,** *98*, 113-9.
13. Kumar, V. A.; Shi, S.; Wang, B. K.; Li, I. C.; Jalan, A. A.; Sarkar, B.; Wickremasinghe, N. C.; Hartgerink, J. D., Drug-triggered and cross-linked self-assembling nanofibrous hydrogels. *J Am Chem Soc* **2015,** *137* (14), 4823-30.

14. Kumar, V. A.; Taylor, N. L.; Shi, S.; Wang, B. K.; Jalan, A. A.; Kang, M. K.; Wickremasinghe, N. C.; Hartgerink, J. D., Highly angiogenic peptide nanofibers. *ACS Nano* **2015,** *9* (1), 860-8.
15. Kumar, V. A.; Taylor, N. L.; Shi, S.; Wickremasinghe, N. C.; D'Souza, R. N.; Hartgerink, J. D., Self-assembling multidomain peptides tailor biological responses through biphasic release. *Biomaterials* **2015,** *52*, 71-8.
16. Kumar, V. A.; Wang, B. K.; Kanahara, S. M., Rational design of fiber forming supramolecular structures. *Exp Biol Med (Maywood)* **2016,** *241* (9), 899-908.
17. Harbour, V.; Casillas, C.; Siddiqui, Z.; Sarkar, B.; Sanyal, S.; Nguyen, P.; Kim, K. K.; Roy, A.; Iglesias-Montoro, P.; Patel, S.; Podlaski, F.; Tolias, P.; Windsor, W.; Kumar, V., Regulation of Lipoprotein Homeostasis by Self-Assembling Peptides. *ACS Applied Bio Materials* **2020,** *3* (12), 8978-8988.
18. Leach, D. G.; Dharmaraj, N.; Piotrowski, S. L.; Lopez-Silva, T. L.; Lei, Y. L.; Sikora, A. G.; Young, S.; Hartgerink, J. D., STINGel: Controlled release of a cyclic dinucleotide for enhanced cancer immunotherapy. *Biomaterials* **2018,** *163*, 67-75.
19. Li, I. C.; Moore, A. N.; Hartgerink, J. D., "Missing Tooth" Multidomain Peptide Nanofibers for Delivery of Small Molecule Drugs. *Biomacromolecules* **2016,** *17* (6), 2087-2095.
20. Sarkar, B.; Nguyen, P. K.; Gao, W.; Dondapati, A.; Siddiqui, Z.; Kumar, V. A., Angiogenic Self-Assembling Peptide Scaffolds for Functional Tissue Regeneration. *Biomacromolecules* **2018,** *19* (9), 3597-3611.
21. Du, X.; Zhou, J.; Shi, J.; Xu, B., Supramolecular Hydrogelators and Hydrogels: From Soft Matter to Molecular Biomaterials. *Chem Rev* **2015,** *115* (24), 13165-307.
22. Behrendt, R.; White, P.; Offer, J., Advances in Fmoc solid-phase peptide synthesis. *J Pept Sci* **2016,** *22* (1), 4-27.
23. Fields, G. B., Introduction to peptide synthesis. *Curr Protoc Protein Sci* **2002,** *Chapter 18*, Unit 18 1.
24. Nguyen, P. K.; Gao, W.; Patel, S. D.; Siddiqui, Z.; Weiner, S.; Shimizu, E.; Sarkar, B.; Kumar, V. A., Self-Assembly of a Dentinogenic Peptide Hydrogel. *ACS Omega* **2018,** *3* (6), 5980-5987.
25. Nguyen, P. K.; Sarkar, B.; Siddiqui, Z.; McGowan, M.; Iglesias-Montoro, P.; Rachapudi, S.; Kim, S.; Gao, W.; Lee, E.; Kumar, V. A., Self-Assembly of an Anti-Angiogenic Nanofibrous Peptide Hydrogel. *ACS Appl. Bio Mater.* **2018,** *1* (3), 865-870.
26. Nguyen, P. K.; Sarkar, B.; Siddiqui, Z.; McGowan, M.; Iglesias-Montoro, P.; Rachapudi, S.; Kim, S.; Gao, W.; Lee, E. J.; Kumar, V. A., Self-Assembly of an Antiangiogenic Nanofibrous Peptide Hydrogel. *ACS Applied Bio Materials* **2018,** *1* (3), 865-870.
27. Sarkar, B.; Siddiqui, Z.; Kim, K. K.; Nguyen, P. K.; Reyes, X.; McGill, T. J.; Kumar, V. A., Implantable anti-angiogenic scaffolds for treatment of neovascular ocular pathologies. *Drug Deliv Transl Res* **2020**.
28. Sarkar, B.; Siddiqui, Z.; Nguyen, P. K.; Dube, N.; Fu, W.; Park, S.; Jaisinghani, S.; Paul, R.; Kozuch, S. D.; Deng, D.; Iglesias-Montoro, P.; Li, M.; Sabatino, D.; Perlin, D. S.; Zhang, W.; Mondal, J.; Kumar, V. A., Membrane-Disrupting

Nanofibrous Peptide Hydrogels. *ACS Biomaterials Science & Engineering* **2019,** *5* (9), 4657-4670.
29. Kim, K. K.; Siddiqui, Z.; Patel, M.; Sarkar, B.; Kumar, V. A., A self-assembled peptide hydrogel for cytokine sequestration. *J Mater Chem B* **2020,** *8* (5), 945-950.
30. Lopez-Silva, T. L.; Leach, D. G.; Azares, A.; Li, I. C.; Woodside, D. G.; Hartgerink, J. D., Chemical functionality of multidomain peptide hydrogels governs early host immune response. *Biomaterials* **2020,** *231*, 119667.
31. Dong, H.; Paramonov, S. E.; Aulisa, L.; Bakota, E. L.; Hartgerink, J. D., Self-assembly of multidomain peptides: balancing molecular frustration controls conformation and nanostructure. *J Am Chem Soc* **2007,** *129* (41), 12468-72.
32. Webber, M. J.; Appel, E. A.; Meijer, E. W.; Langer, R., Supramolecular biomaterials. *Nat. Mater.* **2016,** *15* (1), 13-26.